Structural and Multidisciplinary Optimization
https://doi.org/10.1007/s00158-019-02247-1

BRIEF NOTE

Topology optimization under topologically dependent material uncertainties

Johann Guilleminot[1] · **Alireza Asadpoure**[2] · **Mazdak Tootkaboni**[2]

Received: 9 December 2018 / Revised: 29 January 2019 / Accepted: 22 February 2019

Abstract
A methodology allowing for the algorithmic integration of topologically dependent random fields of material parameters in topology optimization processes is presented. A detailed example is provided to illustrate the methodology step by step.

Keywords Additive manufacturing · Random field · Topology optimization · Uncertainty quantification

1 Introduction

Engineering structures processed by additive manufacturing (AM) techniques are often designed through topology optimization. While AM has proven very effective in producing parts with complex shapes, it is known to introduce a large scatter at the microstructural level, resulting in high levels of uncertainties that eventually propagate across scales (see, *e.g.*, Hu and Mahadevan (2017)). This variability remains a major obstacle to the widespread adoption of AM-produced parts and has fostered the development of topology optimization under uncertainty in recent years. Frameworks currently available involve the definition of material uncertainties on the initial geometry, typically a simple (*e.g.*, rectangular) domain (Chen et al. 2010; Lazarov et al. 2012). This definition may, however, become less relevant as the design iterations go on. More specifically, material uncertainties that would be generated at a given iteration exhibit preferred correlation paths (along existing arches, for example) that cannot be accounted for if the definition of the random field is not updated on the fly. This updating turns out to be very challenging for commonly employed techniques (such as Karhunen-Loève expansions) that require the covariance operator to be defined *a priori*. In particular, the fact that the underlying geometry is iteration dependent (and thus, unknown in advance) and generally nonconvex constitutes a severe obstacle.

This note aims to advance a computational approach enabling the integration of topologically dependent fields of material uncertainties *within* topology optimization. The topology optimization framework is introduced in Section 2. The stochastic approach is presented in Section 3. An illustrative example is finally provided in Section 4.

2 Framework for topology optimization

We propose to proceed following a two-step approach:

- first, deterministic topology optimization with no material uncertainties is performed. The purpose of this initial step is to obtain a *prior optimized configuration*, that meets the typical manufacturability constraints (*e.g.*, minimum length scale).
- second, topology optimization integrating random fields of material properties is performed to compute a *posterior optimized configuration* accounting for the uncertainties that would be generated by the AM technique, should the part be processed at the current iteration of the optimization process.

Responsible Editor: Erdem Acar

✉ Johann Guilleminot
johann.guilleminot@duke.edu

Alireza Asadpoure
aasadpoure@umassd.edu

Mazdak Tootkaboni
mtootkaboni@umassd.edu

[1] Department of Civil and Environmental Engineering, Duke University, Durham, NC, USA

[2] Department of Civil and Environmental Engineering, University of Massachusetts Dartmouth, Dartmouth, MA, USA

Published online: 04 March 2019

Without loss of generality, the topology optimization problem is defined as

$$\min_{\boldsymbol{\phi}} f_0(\boldsymbol{\phi}) \quad \text{s.t.} f_i(\boldsymbol{\phi}) \leq 0\,, \quad 1 \leqslant i \leqslant n_c\,, \tag{1}$$

where f_0 and f_i denote the objective function and the i^{th} constraint, $\boldsymbol{\phi} = \{\phi_i\}_{i=1}^{n_\phi}$ is the vector of design variables defining the topology over the design domain, $D \subset \mathbb{R}^d$, which is typically discretized with a dense mesh of finite elements $\{D_e\}_e$. The goal then is to identify a combination of solid/void elements (a topology) that minimizes the objective function. With upwards of a few thousands design variables, this identification rapidly becomes computationally infeasible if performed in discrete space. A transformation to continuous space that allows for the use of efficient gradient-based (GB) optimizers is therefore essential for solving topology optimization problems with a reasonable computational cost (Sigmund 2011). One way to arrive at such a transformation is to combine the density approach (see, *e.g.*, Sigmund and Maute (2013) for a review) with the Simplified Isotropic Material with Penalization (SIMP) method (Bendsøe 1989; Zhou and Rozvany 1991), where the modulus of element e, E_e, is written as: $E_e = E_{min} + \rho_e^p(E - E_{min})$, where $0 < E_{min} \ll 1$, $\rho_e \in [0,1]$ is the element "density", p the penalization parameter and E the modulus of the base material. The cases $\rho_e = 0$ and $\rho_e = 1$ correspond to void and solid elements, respectively. To avoid numerical instabilities and to impose a minimum length-scale of size $2r_m$ on the developed features, we use the Heaviside projection method (Guest et al. 2004) and write ρ_e as

$$\rho_e(\boldsymbol{\phi}) = 1 - \exp(-\beta\mu_e(\boldsymbol{\phi})) + \mu_e(\boldsymbol{\phi})\exp(-\beta), \tag{2}$$

where β is the shape parameter in the projection and μ_e is defined as $\mu_e(\boldsymbol{\phi}) = (\sum_{i=1}^{n_\phi}\phi_i w_i^e)/(\sum_{i=1}^{n_\phi} w_i^e)$, with $w_i^e = \max\{0, r_m - \|\boldsymbol{x}_e - \boldsymbol{x}_{\phi_i}\|\}$, $\boldsymbol{x}_{\phi_i}$ the coordinate of the design variable ϕ_i and $\boldsymbol{x}_e$ the coordinate of the centroid of element e.

For the sake of illustration in this note, we focus on weight minimization under a minimum stiffness constraint, that is, $f_0 = \int_D \rho(\boldsymbol{x})dD$, where the density field ρ is a piecewise function with $\rho(\boldsymbol{x} \in D_e) = \rho_e(\boldsymbol{\phi})$. The constraints take the form $f_i = \phi_i - 1$ and $f_{n_\phi+i} = -\phi_i$ for $1 \leqslant i \leqslant n_\phi$, and $f_{2n_\phi+1} = \boldsymbol{f}^T\boldsymbol{u}(\boldsymbol{\phi}) - C^*$, where $\boldsymbol{f}$ and $\boldsymbol{u}$ are respectively the applied force and displacement vectors, and C^* is the required minimum stiffness. In the presence of uncertainty, the term $\boldsymbol{f}^T\boldsymbol{u}$ in $f_{2n_\phi+1}$ is replaced by $\mathbb{E}\{\boldsymbol{f}^T\boldsymbol{u}\} + K\sigma\{\boldsymbol{f}^T\boldsymbol{u}\}$, where $K > 0$ is a parameter balancing the contributions, and $\mathbb{E}$ and σ denote the operators of mathematical expectation and standard deviation, respectively (see, *e.g.*, Asadpoure et al. 2011; Tootkaboni et al. 2012).

3 Defining random fields on nonconvex domains

In this section, we describe the methodology enabling the generation of samples of material properties at a given iteration of the optimization process. To this aim, let $\Omega^{\text{iter}} \subseteq D$ be the indexing domain for the random field of interest at a specific iteration. Without loss of generality, we consider the case $d = 2$ and a domain $D = [0, L_1] \times [0, L_2]$ hereinafter. The process of performing topology optimization under uncertainty entails modeling and sampling a random field of material parameters denoted by $\{\boldsymbol{P}(\boldsymbol{x}), \boldsymbol{x} \in \Omega^{\text{iter}}\}$, defined on a probability space $(\Theta, \mathcal{F}, \mathcal{P})$ and with values in $\mathcal{S} \subset \mathbb{R}^p$. For the particular case where either the objective or the constraints involve the compliance, the aforementioned random field typically gathers some stochastic elastic parameters (such as the Young's modulus). Since these parameters take values in (semi-)bounded sets, the random field is non-Gaussian (see, *e.g.*, Soize 2006; Grigoriu 2010) and is presently modeled as a translation random field:

$$\boldsymbol{P}(\boldsymbol{x}) = T(\boldsymbol{\Xi}(\boldsymbol{x}), \boldsymbol{x})\,, \quad \forall\, \boldsymbol{x} \in \Omega^{\text{iter}}\,, \tag{3}$$

where T is a nonlinear transport map and $\{\boldsymbol{\Xi}(\boldsymbol{x}), \boldsymbol{x} \in \mathbb{R}^d\}$ is a normalized $\mathbb{R}^q$-valued Gaussian random field with independent components. The spatial dependence of T allows for the introduction of spatially varying (*e.g.*, mean and/or variance) parameters for the non-Gaussian field, if necessary. Methodologies to construct optimal transport maps for non-Gaussian fields can be found in Soize (2006) and Staber and Guilleminot (2017) for linear constitutive models. Below, we focus on the geometrically consistent definition and random generation of the reference Gaussian field.

The approach pursued in this work relies on the fact that a Gaussian random field exhibiting a Matérn-type correlation function can be interpreted as the stationary solution of the following stochastic partial differential equation (SPDE): $\left(\kappa^2 - \langle\nabla, \nabla\rangle\right)^{\alpha/2}\boldsymbol{\Xi}(\boldsymbol{x}) = \dot{\mathcal{W}}(\boldsymbol{x}), \quad \boldsymbol{x} \in \mathbb{R}^d$, where κ is a parameter, $\langle\cdot,\cdot\rangle$ is the Euclidean inner product, ∇ is the nabla operator and $\{\dot{\mathcal{W}}(\boldsymbol{x}), \boldsymbol{x} \in \Omega^{\text{iter}}\}$ is the spatial normalized Gaussian white noise (Whittle 1954; Lindgren et al. 2011). The exponent α is a key modeling parameter that governs the mean square differentiability of the solution (and thus, the smoothness of realizations, for instance). The anisotropic version of the SPDE reads as

$$\left(\kappa^2 - \langle\nabla, [H(\boldsymbol{x})]\nabla\rangle\right)^{\alpha/2}\boldsymbol{\Xi}_j(\boldsymbol{x}) = \dot{\mathcal{W}}(\boldsymbol{x})\,, \tag{4}$$

where $\boldsymbol{x} \mapsto [H(\boldsymbol{x})]$ is called the diffusion field (Fuglstad et al. 2015).

The central idea in this note is to define the diffusion field on the fly, at every iteration of the optimization algorithm.

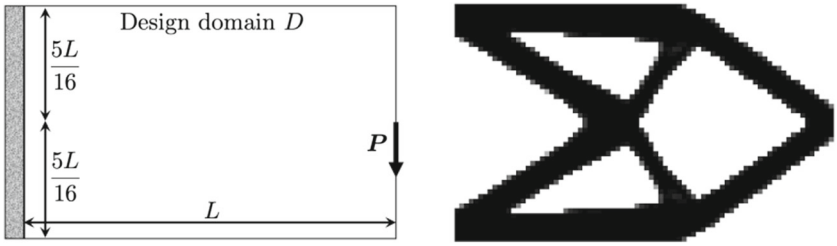

Fig. 1 Geometry and boundary conditions for the cantilever beam (left) and its deterministic optimized design (right)

To this aim, a set of d elementary problems is introduced by considering the Laplace problem

$$\triangle \Psi(\boldsymbol{x}) = 0\,, \quad \forall\, \boldsymbol{x} \in \Omega^{\text{iter}}\,, \tag{5}$$

with boundary conditions written in operator form as $B^{(i)}\{\Psi\}$, with $1 \leqslant i \leqslant d$. The scalar solution to (5) satisfying the boundary condition $B^{(i)}\{\Psi\}$ is denoted by $\boldsymbol{x} \mapsto \Psi_i(\boldsymbol{x})$. The definition of $B^{(i)}$ is problem-specific and must ensure that the gradient of the solution fields represent privileged directions over Ω^{iter} (see below). Let ∂D and $\partial\Omega^{\text{iter}}$ be the boundaries of domains D and Ω^{iter}, and consider the decomposition $\partial D = \cup_{j=1}^{4} \partial D_j$, where $\partial D_1 = \{\boldsymbol{x} \in D \,|\, x_1 = 0\}$, $\partial D_2 = \{\boldsymbol{x} \in D \,|\, x_1 = L_1\}$, $\partial D_3 = \{\boldsymbol{x} \in D \,|\, x_2 = 0\}$ and $\partial D_4 = \{\boldsymbol{x} \in D \,|\, x_2 = L_2\}$. Upon assuming that $\partial\Omega^{\text{iter}} \cap \partial D_j \neq \emptyset$ for $1 \leqslant j \leqslant 4$, the boundary condition operator $B^{(i)}$ can be defined, for instance, by imposing $\Psi(\boldsymbol{x}) = 0$ on $\partial\Omega^{\text{iter}} \cap \partial D_{2i-1}$, $\Psi(\boldsymbol{x}) = 1$ on $\partial\Omega^{\text{iter}} \cap \partial D_{2i}$, and $\langle \nabla\Psi(\boldsymbol{x}), \boldsymbol{n}(\boldsymbol{x})\rangle = 0$ on $\partial\Omega^{\text{iter}} \setminus (\partial D_{2i-1} \cup \partial D_{2i})$, with $\boldsymbol{n}(\boldsymbol{x})$ the outward pointing unit normal vector at point $\boldsymbol{x}$. The solutions of the Laplace problems are next used to construct vector fields $\{\boldsymbol{x} \mapsto \boldsymbol{e}^i(\boldsymbol{x})\}_{i=1}^{d}$ corresponding to the normalized velocities of the potential flows:

$$\boldsymbol{e}^i(\boldsymbol{x}) = \nabla\Psi_i(\boldsymbol{x})/\|\nabla\Psi_i(\boldsymbol{x})\|,\,, \quad \forall\, \boldsymbol{x} \in \Omega^{\text{iter}}\,. \tag{6}$$

In more general situations where not all boundaries of D intersect with $\partial\Omega^{\text{iter}}$, a possible strategy consists of defining one vector field, say $\boldsymbol{x} \mapsto \boldsymbol{e}^1(\boldsymbol{x})$, by solving a Laplace problem under a specifically defined operator $B^{(1)}$, and to construct the field $\boldsymbol{x} \mapsto \boldsymbol{e}^2(\boldsymbol{x})$ through an orthogonality condition, $\langle \boldsymbol{e}^1(\boldsymbol{x}), \boldsymbol{e}^{(2)}(\boldsymbol{x})\rangle = 0$. The vector fields $\{\boldsymbol{x} \mapsto \boldsymbol{e}^i(\boldsymbol{x})\}_{i=1}^{d}$ thus obtained represent natural correlation paths on the geometry, suggesting to define the diffusion matrix $[H(\boldsymbol{x})]$ as

$$[H(\boldsymbol{x})] = \sum_{1 \leqslant i \leqslant d} \lambda_i\, \boldsymbol{e}^i(\boldsymbol{x}) \otimes \boldsymbol{e}^i(\boldsymbol{x})\,, \quad \forall\, \boldsymbol{x} \in \Omega^{\text{iter}}, \tag{7}$$

where the parameters $\{\lambda_i > 0\}_{i=1}^{d}$ control anisotropy in terms of correlation ranges. It should be noticed that these parameters can be made spatially dependent to increase modeling flexibility. Note that standard models (defined on the initial configuration) can trivially be recovered using $e^i_j(\boldsymbol{x}) = \delta_{ij}$, with δ the Kronecker delta.

As proposed in Lindgren et al. (2011), the Gaussian solution to the SPDE defined on a bounded domain and subjected to Neumann boundary conditions can be obtained, for $\alpha = 2$, by using a Galerkin method (note that the solution for arbitrary integer orders $\mathbb{N}_{>2}$ can be obtained by a recursion formula). The approximation reads as $\Xi(\boldsymbol{x}) = \sum_{i=1}^{N} \eta_i \psi_i(\boldsymbol{x})$, where $\{\psi_i\}_{i=1}^{N}$ is the finite element basis consisting of piecewise linear functions. The discretized form involves the $(N \times N)$ matrices $[M]$ and $[G]$ with entries $M_{ij} = \int_{\Omega^{\text{iter}}} \psi_i(\boldsymbol{x})\psi_j(\boldsymbol{x})d\boldsymbol{x}$ and $G_{ij} = \int_{\Omega^{\text{iter}}} \langle \nabla\psi_i(\boldsymbol{x}), [H(\boldsymbol{x})]\nabla\psi_j(\boldsymbol{x})\rangle d\boldsymbol{x}$ for $1 \leqslant i, j \leqslant N$. It can be shown (see Lindgren et al. 2011) that the vector of stochastic nodal values satisfies $\boldsymbol{\eta} \sim \mathcal{N}(\boldsymbol{0}, [\Sigma])$. The random vector $\boldsymbol{\eta}$ can then be defined as the solution of the linear system $[L]\boldsymbol{\eta} = \boldsymbol{g}$, where $\boldsymbol{g} \sim \mathcal{N}(\boldsymbol{0}, [I_N])$ and the upper triangular $[L]$ is such that the sparse precision matrix reads as $[Q] = [L]^{\mathsf{T}}[L]$.

4 Application

In order to illustrate the proposed framework, we now consider topology optimization of a cantilever beam (see

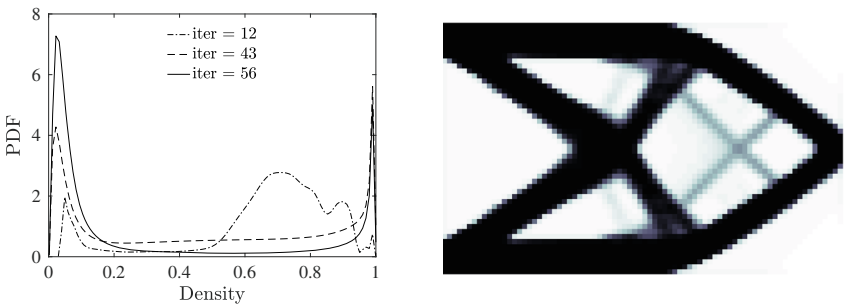

Fig. 2 Deterministic topology optimization: PDF of the density at different iterations (left) and prior configuration at iter = 56 (right)

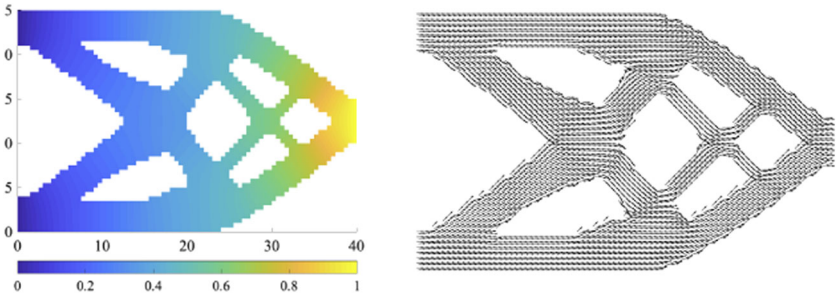

Fig. 3 Left: $\boldsymbol{x} \mapsto \Psi_1(\boldsymbol{x})$. Right: $\boldsymbol{x} \mapsto \boldsymbol{e}^1(\boldsymbol{x})$

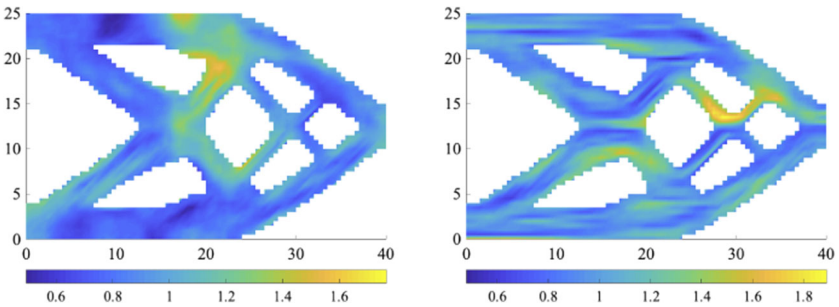

Fig. 4 One sample of the Young's modulus random field obtained for the isotropic (left) and anisotropic (right) cases

Fig. 5 Posterior configurations obtained for the isotropic (left) and anisotropic (right) cases for $K = 3$

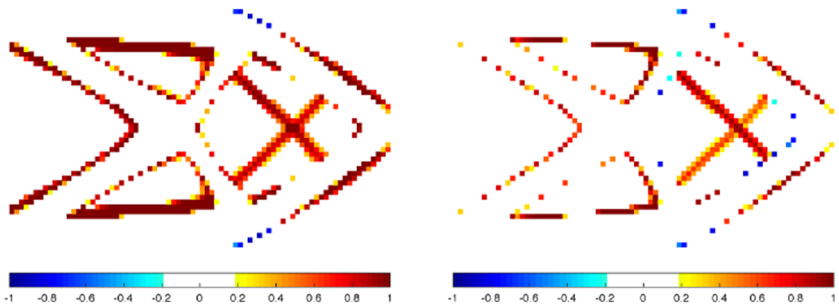

Fig. 6 Difference between the optimized solutions generated with locally isotropic (left) and anisotropic (right) kernels and the deterministic solution

Fig. 1 for the geometry of the design domain and the boundary conditions). We set $C^* = 1600P/EL$, discretize the domain into 80×50 quad elements and choose $r_m = h\sqrt{2}/2$, with h size of the finite elements. The modified method of moving asymptotes (Svanberg 1987) is used as the GB optimizer with p and β suggested in Guest et al. (2011). The deterministic optimized solution is shown in Fig. 1. In the presence of uncertainty in material property, the statistics of interest and their sensitivities are computed by the Monte Carlo and adjoint methods.

Following the first step of the methodology, the probability density function of the density field along design iterations is used to track early stages where a fully connected topology (characterized by pronounced bimodality) is forming, and the topology obtained after 56 iterations is selected (see Fig. 2).

For the sake of illustration, we consider the case of a stochastic Young's modulus such that $E(\boldsymbol{x})$ follows a Gamma distribution, $E(\boldsymbol{x}) \sim \mathcal{G}(k, \theta)$, for any $\boldsymbol{x}$ fixed in Ω^{iter}, with k and θ the scale and shape parameters of the distribution. These parameters are chosen such that the mean and coefficient of variation of the Young's modulus are given by $\underline{E} = 1$ and $\delta_E = 0.2$. The solution to an elementary problem is shown, together with its gradient, in Fig. 3.

The fields $\{\boldsymbol{x} \mapsto \boldsymbol{e}^i(\boldsymbol{x})\}_{i=1}^2$ thus obtained are next used to construct the diffusion field given by (7). In order to demonstrate the impact of the correlation structure and in particular, the influence of anisotropy, two configurations are tested: $\lambda_1 = \lambda_2 = 0.2$ (isotropic structure) and $(\lambda_1, \lambda_2) = (0.2, 0.0001)$ (anisotropic structure). The parameter κ is set to 0.15. Samples obtained for these configurations are shown in Fig. 4, which qualitatively illustrates the impact of the diffusion on the realizations.

It should be noted that the same realization of $\boldsymbol{g}$ was used for both the isotropic and anisotropic case, for comparison purposes. The final posterior topologies obtained starting from the prior topology in Fig. 2 and the parameters given above are shown in Fig. 5.

The impact of an anisotropic correlation structure, likely to be induced by the directional preferences of AM, can be noticed (see Fig. 6).

5 Conclusion

A methodology allowing for the robust integration of topologically dependent material uncertainties within topology optimization was presented. The impact on the optimized configuration is shown to be significant, even for contained fluctuations in elastic properties.

Funding information JG and MT received financial support from the National Science Foundation under Grants No. CMMI-1726403 and CMMI-1401575, respectively. AA also acknowledges support from UMass Dartmouth College of Engineering.

Compliance with ethical standards

Conflict of interest The authors declare that there is no conflict of interest.

Replication of results All the necessary data to reproduce the results reported here are provided in Section 4.

References

Asadpoure A, Tootkaboni M, Guest JK (2011) Comput Struct 89(11-12):1131
Bendsøe MP (1989) Struct Optim 1(4):193
Chen S, Chen W, Lee S (2010) Struct Multidiscip Optim 41(4):507
Fuglstad GA, Lindgren F, Simpson D, Rue H (2015) Stat Sin 25:115
Grigoriu M (2010) J Comput Phys 229(22):8406. https://doi.org/10.1016/j.jcp.2010.07.023
Guest JK, Prévost JH, Belytschko TB (2004) Int J Numer Methods Eng 61(2):238
Guest JK, Asadpoure A, Ha SH (2011) Struct Multidiscip Optim 44(4):443
Hu Z, Mahadevan S (2017) Scr Mater 135:135
Lazarov BS, Schevenels M, Sigmund O (2012) Struct Multidiscip Optim 46(4):597
Lindgren F, Rue H, Lindstrôm J (2011) J Royal Stat Soc: Ser B (Stat Methodol) 73(4):423
Sigmund O (2011) Struct Multidiscip Optim 43(5):589
Sigmund O, Maute K (2013) Struct Multidiscip Optim 48(6):1031
Soize C (2006) Comput Methods Appl Mech Eng 195(1):26
Staber B, Guilleminot J (2017) Compt R - Mecanique 345(6):399
Svanberg K (1987) Int J Numer Methods Eng 24(2):359
Tootkaboni M, Asadpoure A, Guest JK (2012) Comput Methods Appl Mech Eng 263:201–204
Whittle P (1954) Biometrika 41(3-4):434
Zhou M, Rozvany GIN (1991) Comput Methods Appl Mech Eng 89(1-3):309